# Estimation of Intrinsic and Reflex Contributions to Muscle Dynamics: A Modeling Study

Eric J. Perreault*, *Member, IEEE*, Patrick E. Crago, *Member, IEEE*, and Robert F. Kirsch, *Member, IEEE*

*Abstract*—This work evaluated system identification-based approaches for estimating stretch reflex contributions to muscle dynamics. Skeletal muscle resists externally imposed stretches via both intrinsic stiffness properties of the muscle and reflexively mediated changes in muscle activation. To separately estimate these intrinsic and reflex components, system identification approaches must make several assumptions. We examined the impact of making specific structural assumptions about the intrinsic and reflex systems on the system identification accuracy. In particular, we compared an approach that made specific parametric assumptions about the reflex and intrinsic subsystems to another that assumed more general nonparametric subsystems. A simulation-based approach was used so that the "true" characters of the intrinsic and reflex systems were known; the identification methods were judged on their abilities to retrieve these known system properties. Identification algorithms were tested on three experimentally based models describing the stretch reflex system. Results indicated that the assumed form of the intrinsic and reflex systems had a significant impact on the stiffness separation accuracy. In general, the algorithm incorporating nonparametric subsystems was more robust than the fully parametric algorithm because it had a more general structure and because it provided a better indication of the appropriateness of the assumed structure.

*Index Terms*—Muscle, simulation, stiffness, stretch reflex, system identification.

## I. INTRODUCTION

THIS paper describes a modeling study that evaluated system identification-based approaches for noninvasively estimating the stretch reflex contribution to muscle dynamics. Skeletal muscle resists externally imposed stretches due to stiffness properties of the muscle itself and to reflexively mediated changes in muscle activation. Although the stretch reflex has been widely studied, its role during typical motor tasks remains a topic of much debate [1]–[3]. This controversy stems in part from difficulties associated with quantifying the reflex response *in vivo* and separating reflex contributions to the stretch response from intrinsic muscle properties and voluntary interventions. A reliable method for quantifying stretch reflex contributions to motor output would help elucidate the role of

these reflexes during typical motor tasks in both able-bodied individuals and individuals with motor pathologies such as tremor, spasticity, and paresis from various etiologies.

Until recently, reflex responses in intact, unimpaired human subjects could be studied only through the use of methods that effectively deafferented a muscle, including vibration [4], [5], ischemia [5], [6], and electrical stimulation [7], [8]. In these studies, reflex contributions are defined as the change in motor output between the reflexive and areflexive states. These methods have shown that reflex contributions can be significant under many conditions, but they suffer from several important limitations. First, the techniques used to suppress the reflex response are not completely isolated to stretch reflex mechanisms, but rather may also have unnatural side-effects (e.g., altered motoneuron properties during ischemia and changes in intrinsic muscle stiffness during vibration). Second, even if a completely selective removal of the stretch reflex were possible, it would be difficult to interpret the differences between the intact and areflexive states. Stretch reflex responses are thought to depend upon a balance between a large number of descending and segmental inputs. Simple removal of one class of these inputs will result in a change in the stretch response, but replacement of the suppressed inputs to match experimental conditions (e.g., joint torque) will cause a change in the normal balance of the various systems, and a corresponding change in the stretch response. Thus, effective deafferentation methods provide only a relatively crude reflection of reflex behavior at discrete operating points.

Recently, several methods have been proposed for studying the stretch reflex noninvasively in completely intact systems. These methods rely on signal processing and the known delay in the stretch reflex system, rather than physical disruption of the system, to separate reflexive contributions to motor output from intrinsic contributions. These methods generally assume that the intrinsic and reflex responses to stretch sum linearly. This simplification ignores the nonlinear behavior of muscle and motoneurons [9]–[11], yet provides a functionally useful definition for characterizing the reflex response for small displacements about a steady operating point [12], [13]. Time delay methods using sinusoidal perturbations [12], [13], pulse perturbations [14], [15], and stochastic perturbations [16], [17] have been employed. The latter use the tools of nonlinear system identification to characterize the intrinsic and reflex dynamics from a single experimental trial and hence, provide an experimentally efficient tool for studying reflex responses. In addition, the system identification approach provides a quantitative description of the intrinsic and reflex dynamics that can be incorporated into mathematical models of motor behavior. These attractive

characteristics of system identification-based approaches led us to further investigate their use for estimating the relative mechanical contributions of intrinsic and reflex properties.

Although the system identification-based methods are appealing, they are not magic. In order to separate intrinsic and reflex components on the basis of time delay, any system identification approach must make several assumptions. First, the duration of the reflex delay must be known or estimated in some way. Second, and most importantly, some assumption regarding the *structures* of the intrinsic and reflex (sensor properties, central processing, and muscle response to reflex activation) systems must be made. Making this assumption is unavoidable because the same input variables (e.g., muscle length and its derivatives) excite both the intrinsic muscle properties and the reflex system. Furthermore, the intrinsic and reflex components will be at least partially correlated, so their common component could be attributed to an arbitrary combination of intrinsic and reflex properties depending on what is assumed for the reflex structure. Unfortunately, this means that errors in the relative distribution of intrinsic and reflex components may not be reflected in the goodness of fit.

In this study, we examined the impact of making different assumptions about the structures of the intrinsic and reflex systems. In particular, we compared an approach [17] that made specific parametric assumptions about the form of the subsystems to another approach that assumed more general nonparametric subsystems [16]. We used a simulation-based approach so that the "true" characters of the intrinsic and reflex systems were known—the performance of the identification methods was judged on their abilities to retrieve these known system properties. Several different experimentally-based model structures for the "true" system were used in different simulations. We evaluated the ability of the different system identification approaches to accurately separate the intrinsic and reflex stiffness components for each of these models. The results of these simulations indicate that the assumed form of the intrinsic and reflex systems can have a significant impact on the accuracy of the stiffness separation procedures. In general, the algorithm incorporating nonparametric subsystems was more robust than the fully parametric algorithm because it had a more general structure and because it provided a better indication of the appropriateness of the assumed identification model.

Portions of this work have been presented previously [18].

## II. METHODS

### A. Identification Algorithms

System identification algorithms can be characterized broadly into parametric and nonparametric techniques [19]. Parametric algorithms describe the system under study using a specific set of equations, usually with a minimal set of parameters. Often, these equations are constructed from first principles or from previous empirical findings. The goal of parametric identification is to estimate the parameters of this equation set. In contrast, nonparametric algorithms make few assumptions about the system under study and typically do not require *a priori* knowledge of the equations describing the system response. The goal of nonparametric identification is to estimate points on the unparameterized system response curves, such as impulse response functions (IRFs) for linear systems or kernels for nonlinear systems.

Three separate identification algorithms were implemented in this study. The first method was a commonly used [6], [20]–[22] linear parametric identification algorithm that modeled the whole joint response without distinguishing between reflex and intrinsic contributions. This provided the baseline results against which to compare the performance of two additional algorithms that were designed to separately identify reflex and intrinsic contributions to total joint dynamics. Each algorithm estimated the *dynamic stiffness* of a joint, which is the relationship between externally imposed joint displacements and the corresponding joint torques, to fully characterize the mechanical properties of the joint.

*1) Method A: Linear Parametric Algorithm:* Method A, a linear parametric estimation algorithm, assumed that dynamic joint stiffness can be modeled by a second-order system(1) containing terms for the inertia $(I)$, viscosity $(B)$, and elastic stiffness $(K)$ of the joint. In (1), $T$ represents joint torque and $\Theta$ represents joint angle. Method A makes no attempt to separate intrinsic contributions from reflex contributions to the dynamic stiffness, but rather lumps them into a single system [Fig. 1(A)] with properties that are expected to change with changes in reflex activation. A "direct" method was used to estimate these parameters. This involves doubly integrating both sides of (1) with a linear integral filter and solving for the parameters of the resulting equation using least squares. Equation (2) shows the double integrator used in this study [17], where $h$ is the sampling interval, $l$ is the length of the integral filter, $z^{-1}$ is the unit delay operator, $\phi(t)$ is the measured torque or displacement to be integrated, and $j = 0, 1, 2$ corresponds to the zeroth, first, or second derivative terms. The $l*h$ product was set to one sample shorter than the simulated reflex delays listed in the *Simulation* section. The use of this integration before parameter estimation avoids the need to differentiate the experimental data, which can be problematic

$$T(t) = I\ddot{\theta}(t) + B\dot{\theta}(t) + K\theta(t) \tag{1}$$

$$\int_{t-lh}^{t} \int_{t_1-lh}^{t_1} \frac{d^j \phi(\tau)}{d\tau^j} \, d\tau \, dt_1$$

$$\approx (1 - z^{-1})^j \cdot \left[ \frac{h}{2}(1 - z^{-1}) \right]^{2-j}$$

$$\cdot (1 + z^{-1} + \cdots + z^{-l+1}) \cdot \phi(t). \tag{2}$$

*2) Method B: Nonlinear Parametric Algorithm:* Method B was a nonlinear parametric identification algorithm first proposed by Zhang and Rymer [17] for characterizing the reflex response of the human elbow. This algorithm assumes that the joint dynamics can be described by the system shown in Fig. 1(B). This model structure was determined *a priori*, based on previous studies of muscle and reflex properties in both humans and animals [23]–[26]. In this model, the intrinsic joint dynamics are represented by (1), while the reflex pathway contains position and velocity dependent components that provide a delayed response $(t_d)$ to an applied joint stretch. Position feedback is modeled by a static gain, $K_d$, and velocity
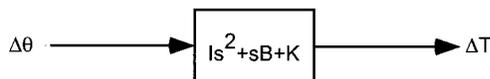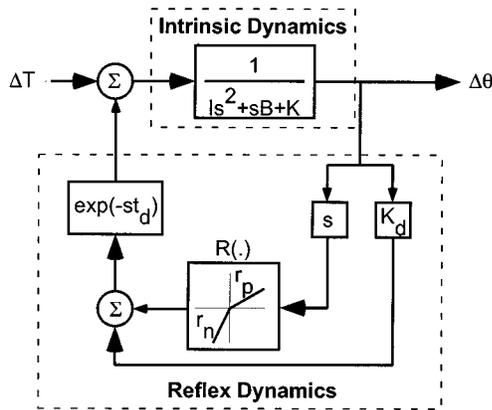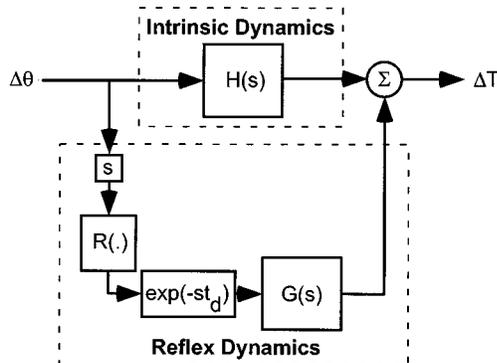
## (A) Method A



## (B) Method B



## (C) Method C



Fig. 1. Joint stiffness structures assumed by each of the system identification algorithms. (A) Method A assumed a second-order system with inertial, viscous, and elastic terms. (B) Method B assumed separate intrinsic and reflex pathways, both which were parameterized. (C) Method C used a block-structured nonparametric algorithm with separate intrinsic and reflex pathways. All components of this assumed structure were estimated nonparametrically.

feedback is modeled by a static nonlinearity with separate gains for positive $(r_p)$ and negative $(r_n)$ stretches. In addition to these parameters identified in the original publication [17], an offset parameter, $\bar{\mu}$, was added to the velocity feedback nonlinearity to account for the shift in the mean reflexively generated torque due to nonequal feedback gains for positive and negative velocities. This additional parameter had little effect on the identification of intrinsic dynamics, but greatly improved the identification accuracy for the reflex parameters. In their study of elbow dynamics, Zhang and Rymer estimated the reflex delay and joint inertia in separate experiments from those used to estimate the remaining model parameters. To mimic this approach, joint inertia and the reflex delay were assumed to be known in this work. Therefore, this model had a total of 6 free parameters. Equation (3) shows the nonlinear delay

differential equation describing the reflex structure shown in Fig. 1(B); $e(t)$ is the error associated with this model. Because this equation is linear in its parameters, these parameters can also be estimated using linear least squares. Again, this was accomplished using the "direct" method outlined above. Each side of (3) was integrated over a period slightly shorter than the reflex delay using (2) and then the model parameters were estimated using linear least squares

$$I\ddot{\theta}(t) + B\dot{\theta}(t) + K\Delta\theta(t) + \begin{bmatrix} r_p, \langle \dot{\theta}(t) > 0 \rangle \\ r_n, \langle \dot{\theta}(t) < 0 \rangle \end{bmatrix} \dot{\theta}(t - t_d)$$
$$+ K_d\Delta\theta(t - t_d) + \bar{\mu} = \Delta T(t) + e(t). \quad (3)$$

*3) Method C: Block Structured Nonlinear Nonparametric Algorithm:* Method C was first used by Kearney *et al.* [16] to characterize reflex responses at the human ankle. This algorithm assumes the existence of separate intrinsic and reflex pathways as well as a specific form for these pathways, but the elements in both pathways remain fully nonparametric. It is therefore less structured than the fully parametric identification of Method B, yet is not fully nonparametric; it falls into the class of block-structured nonparametric algorithms [27]. The structural information assumed by Method C was obtained from a series of experiments on the human ankle [21], [28]. The resulting nonlinear algorithm assumed that the parallel structure of Fig. 1(C) could describe the joint dynamics. In Fig. 1(C), $H(s)$ and $G(s)$ represent linear systems, respectively, describing the areflexive intrinsic stiffness dynamics and the reflex activation dynamics. The delayed reflex dynamics are preceded by a differentiator and a static nonlinearity, $R(\cdot)$, which has been found to closely resemble a half-wave rectifier [28].

This algorithm uses nonparametric IRFs to estimate the intrinsic and reflex dynamics. The separation of these dynamics requires a stiff position servo to control joint displacements and decay of the intrinsic torque response to an instantaneous *externally* imposed displacement before the onset of the reflex response to the same displacement. In other words, the intrinsic dynamics IRF needs to decay before the onset of reflex activity. Numerous studies have shown that, during the application of stochastic perturbations, the stiffness properties of muscles and joints can be described by a system with inertial, viscous and elastic properties [6], [21], [22], [29], [30]. These systems have instantaneous transient responses to applied *displacement* perturbations, allowing the intrinsic and reflex components to be separated in time [14], [15]. The technique for achieving this separation during the application of continuous perturbations is outlined below

1) Estimate the intrinsic dynamics from the measured displacement and torque data using a two-sided IRF [31] that decays before the onset of reflex activity. This is accomplished by solving the discrete convolution equation given below, where $h(k)$ is the nonparametric IRF of length $2N + 1$, $\phi_{xy}(k)$ is the cross-correlation between the measured input and output, and $\phi_{xx}(k)$ is the input auto-correlation

$$\phi_{xy}(k) = \sum_{j=-N}^{N} h(j) \cdot \phi_{xx}(j - k). \quad (4)$$

2) Subtract the torque predicted by the estimated intrinsic dynamics from the measured torque to obtain the reflex torque.

3) Identify the dynamics of the reflex pathway describing the relationship between joint displacements and reflex torque using an iterative Hammerstein identification algorithm [27]. Hammerstein systems consist of a static nonlinearity followed by a linear system, as assumed for the reflex dynamics illustrated in Fig. 1(C). The reflex IRF in this pathway was forced to zero where the intrinsic IRF was allowed to be nonzero, thereby preventing unmodeled intrinsic dynamics from being incorporated into the reflex path. The static nonlinearity was approximated with a tenth-order Chebyschev polynomial.

To allow comparison with the parametric methods, elastic and viscous parameters were fit to the nonparametrically estimated intrinsic stiffness IRFs using a simplex optimization routine (The Mathworks, Natick, MA).

### B. Simulations

Three different models of the stretch reflex response were simulated. They were based on experimental results obtained for the human ankle, the human elbow, and the cat soleus. These models were chosen to illustrate key points regarding system identification of intrinsic and reflex dynamics, not to encompass all possible stretch reflex behaviors. The simulated data from these models were used to test the conditions under which each of the identification algorithms described above could accurately predict the contributions of the intrinsic and reflex systems to the total dynamic stiffness. Each model was simulated with a range of reflex gains, but constant intrinsic properties. The nonlinear identification algorithms were judged on their ability to identify the invariant intrinsic dynamics at all levels of reflex gain. These parameters were used as a succinct measure of success because they were common to all tested algorithms. Errors in their estimation indicate that the intrinsic and reflex pathways were not properly separated but rather that changes in reflex gain influenced the estimation of the intrinsic properties. The linear parametric algorithm was used to summarize how changes in reflex gain affected the net stiffness dynamics.

To emphasize the effects of model structure on the identification process, two simplifications were made during the simulation process that caused the data used in this study to differ from that collected in an actual experiment. First, inertia was eliminated from all simulations, and second, all measurements were assumed to be noise free. Although inertia provides a significant reaction force to imposed displacements of intact joints, its effects are not directly influenced by muscle or reflex activity. Hence, the elimination of inertia yielded a data set affected only by intrinsic and reflex responses, thereby allowing the study to focus on how changes in these factors influence the system identification procedures. In an experimental setting, inertia obviously needs to be identified and the accuracy of its estimation will influence the accuracy of any parametric identification algorithm. Similarly, measurement noise will degrade the performance of both parametric and nonparametric algorithms. The elimination of these confounding factors provides a "best case" scenario for testing the identification algorithms, and allows the

#### TABLE I
#### PARAMETERS FOR ELBOW SIMULATION

| Parameter | Value | Units | Description |
|-----------|-------|-------|-------------|
| I | 0 | kg-m/rad | intrinsic inertia |
| B | 3 | N-m-s/rad | intrinsic viscosity |
| K | 75 | N-m/rad | intrinsic stiffness |
| $t_d$ | 50 | msec | reflex delay |
| $K_d$ | 15 | N-m/rad | reflex stiffness |
| $r_n$ | 0.5 | N-m-s/rad | negative velocity reflex gain |
| $r_p$ | 0.1 | N-m-s/rad | positive velocity reflex gain |

#### TABLE II
#### PARAMETERS FOR ANKLE SIMULATION

| Parameter | Value | Units | Description |
|-----------|-------|-------|-------------|
| I | 0 | kg-m/rad | intrinsic inertia |
| B | 0.8 | N-m-s/rad | intrinsic viscosity |
| K | 130 | N-m/rad | intrinsic stiffness |
| $t_d$ | 46 | msec | reflex delay |
| G | 15 | N-m/s | reflex gain |
| $\xi$ | 0.6 | - | reflex damping |
| $\omega_0$ | 21 | rad/s | reflex resonance |

causes for any limitations in their performance under these ideal conditions to be more readily identified.

*1) Human Elbow Model:* The human elbow model was based on the experimental results of Zhang and Rymer [17]. Fig. 1(B) shows the structure of this model, which matches exactly the assumptions of Method B. Equation (3) provides the dynamics equation for this structure. Typical parameters reported by Zhang and Rymer were used in the simulation. Table I provides the chosen values. Changes in reflex gain were simulated by scaling all gain parameters in the reflex pathway $(K_d, r_p, r_n)$ equally, relative to the nominal values provided in Table I.

*2) Human Ankle Model:* The human ankle model was based on the experimental results of Kearney *et al.* [16]. Fig. 1(C) shows the structure of this model, which exactly matches the assumptions of Method C. For simulation purposes, the linear dynamics were parameterized according to the reported experimental results. The intrinsic stiffness dynamics, $H(s)$, were represented by the second-order system given in (1). The reflex dynamics, $G(s)$, were also shown to be second-order, and were modeled by (5); $G$ represents the reflex gain, $\omega_0$ the natural frequency, and $\xi$ the damping parameter. A half-wave rectifier was used to approximate the static nonlinearity in the reflex path, providing a directionally sensitive reflex response. Table II shows the actual parameters used during these simulations. Note that the structure of the simulated ankle model is very close to that for the simulated elbow model described above. Hence, the choice of these two models allows us to predict how the two chosen classes of identification algorithms behave when the "true" system structure differs only slightly from the estimated structure

$$G(s) = \frac{G}{\left(\frac{s}{\omega_0}\right)^2 + 2\frac{\xi}{\omega_0}s + 1} e^{-st_d}. \qquad (5)$$
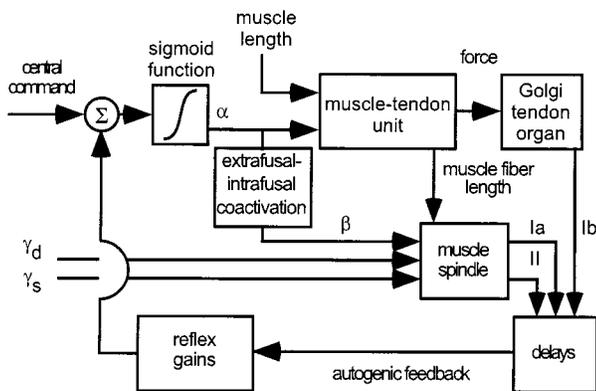
Fig. 2. Cat soleus reflex model. Experimentally based structural model formulated from previously published results. See text.



Fig. 3. Identification results for the human elbow model. (A) The variance accounted for by each identification algorithm. (B) The estimated joint stiffness. (C) The estimated joint viscosity. The thick gray lines in (B) and (C) indicate the simulated intrinsic viscosity and stiffness.

*3) Cat Soleus Model:* The final model used to generate simulated data was a physiologically based structural model of the cat soleus [32]. This model did not explicitly meet the assumptions of any implemented identification algorithm, and hence was used to illustrate how these algorithms behave when used to estimate the dynamics of a plausible reflex system that differs from the implicitly assumed structure. The model was synthesized from previously published experiments on the cat soleus neuromuscular system, and includes descriptions of muscle spindles, Golgi tendon organs, the associated afferents (Ia, II, and IIb), the $\alpha$ motoneuron pool and its branches ($\beta$ innervation), and extrafusal muscle fibers. Fig. 2 illustrates the interconnections between these structures. Parameters for each structure were chosen to match their responses in isolation. Four model parameters were then adjusted so that the entire system fit a portion of the experimental data presented by Nichols and Houk [33]. These parameters were the $\gamma$-motoneuron input and the feedback gains for the groups Ia, Ib, and II fibers. With this fixed set of parameters, the model reproduces soleus stretch reflex behavior over a range of previously reported conditions [33], [34]. In this study, the feedback gains for the groups Ia, Ib, and II fibers were scaled equally to simulate changes in reflex gain for the purposes of evaluating the system identification procedures.

*4) Simulation Parameters:* Stochastic joint angle (or muscle length) perturbations were used as the input to each model to approximately replicate the experiments from which the elbow and ankle model parameters were derived. The input perturbation bandwidth was normalized to the bandwidth of the intrinsic model dynamics, and was chosen to produce an approximately flat torque/force spectrum out to a frequency four times greater than the intrinsic bandwidth. Beyond this point, the simulated model torque/force declined at a rate of 20 dB/decade. The calculations for the intrinsic dynamics bandwidth incorporated the effects of joint inertia, to mimic values that would be obtained experimentally. The resultant model input was sufficient to estimate the intrinsic dynamics of all models in the absence of a reflex response. Changes in reflex gain were simulated by scaling the nominal reflex gain parameters described above, but leaving all other model parameters constant. Intrinsic stiffness parameters remained invariant for all simulated levels of reflex gain. The models were coded in Matlab/Simulink and simulated using
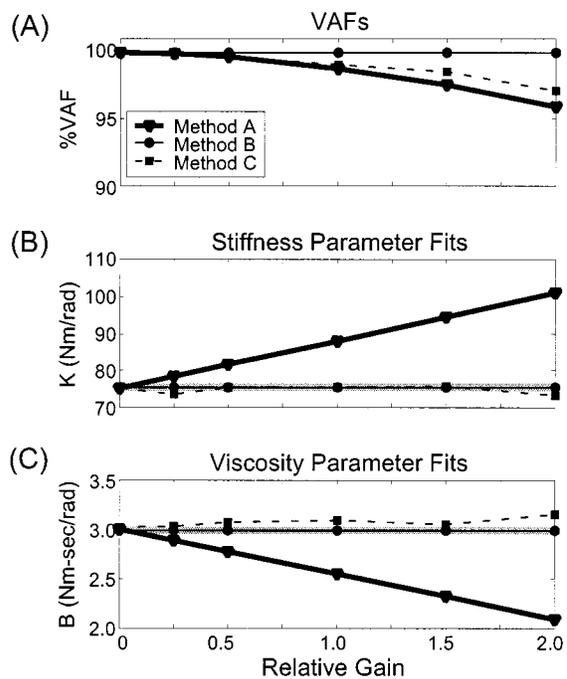
an adaptive stepsize Gear-type integration algorithm, which was forced to output data at equidistant points in time. The resulting sampling rates were 500 Hz for the elbow and ankle data, and 2000 Hz for the cat soleus data.

## III. RESULTS

### A. Elbow Model

Fig. 3 summarizes the ability of each identification algorithm to characterize to simulated elbow system as the reflex gain was varied relative to the nominal parameters reported in Table I. Fig. 3(A) shows the variance accounted for (VAF), Fig. 3(B) the estimated intrinsic stiffness, and Fig. 3(C) the estimated intrinsic viscosity. Note that for Methods B and C, these parameters represent the estimated intrinsic joint properties, whereas for Method A they incorporate both reflex and intrinsic properties and hence, summarize the total joint response. All three algorithms described the simulated elbow torques well, always having a VAF greater than 95% across all reflex gains. In all cases, Method B, which had a structure identical to the simulated system, was the most accurate ($\mathrm{VAF} > 99.5\%$). Method A showed that increased reflex feedback increased the net joint stiffness ($K$) and decreased the net joint viscosity ($B$), which is consistent with numerous experimental reports [6], [8], [12], [13], [33], [35]. Methods B and C both estimated nearly invariant intrinsic joint properties ($K$ and $B$) at changing levels of reflex gain. Again, Method B produced the most accurate estimates. These were within 1.0% of the true parameter values and showed no trend with increasing reflex gain. The intrinsic joint stiffness and viscosity parameters estimated by Method C were accurate to within 2.5% and 6%, respectively. Joint viscosity
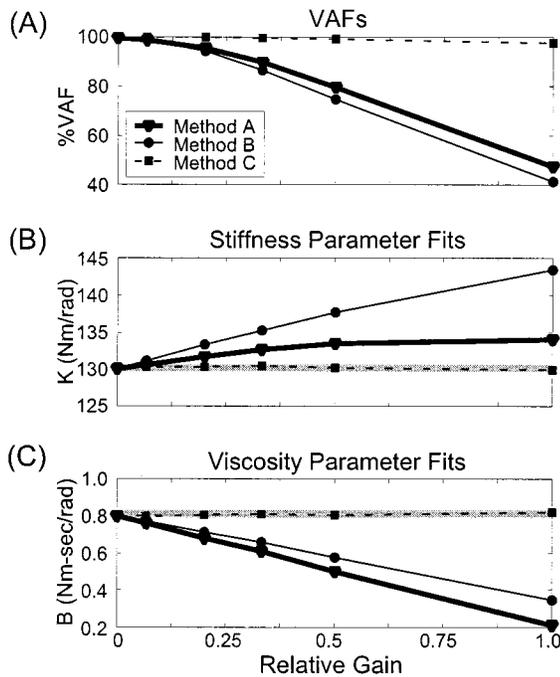
Fig. 4. Identification results for the human ankle model. (A) The variance accounted for by each identification algorithm. (B) The estimated joint stiffness. (C) The estimated joint viscosity. The thick gray lines in (B) and (C) indicate the simulated intrinsic viscosity and stiffness.

was slightly overestimated due to a small but statistically significant increase in estimated viscosity with reflex gain (1.8% per unit of normalized reflex gain; $p < 0.05$) coupled with a statistically insignificant offset ($\Delta \bar{\mu} = 0.8\%; p > 0.1$).

### B. Ankle Model

Fig. 4 summarizes how well the three identification algorithms characterized the simulated ankle system at different levels of reflex gain relative to that reported in Table II. Again, Fig. 4(A) shows the VAF, Fig. 4(B) the estimated intrinsic stiffness, and Fig. 4(C) the estimated intrinsic viscosity. For this simulated system, only Method C accurately described the simulated torques at all levels of reflex gain. This algorithm had greater than 97% VAF for all experimental trials. In contrast, neither Method A nor Method B predicted the torque data at high reflex gains, with VAFs below 80% at a normalized reflex gain of 0.5 and below 50% for a normalized gain of 1.0. Method A showed that increasing the reflex gain in this model also increased total elastic joint stiffness and decreased total joint viscosity, although changes in viscosity dominated the net response. At the experimentally reported levels of reflex gain (normalized gain = 1.0), the stretch reflex increased net elastic joint stiffness by 3% and decreased net viscosity by 73% with respect to the areflexive conditions. Of the algorithms that tried to separately identify intrinsic and reflex dynamics, only Method C accurately estimated constant intrinsic joint dynamics at all levels of reflex gain; stiffness and viscosity parameters remained within 3% of the simulated values for all tested conditions. The intrinsic parameters estimated by Method B varied as a function of reflex gain, indicating that this method was unable to accurately separate intrinsic and
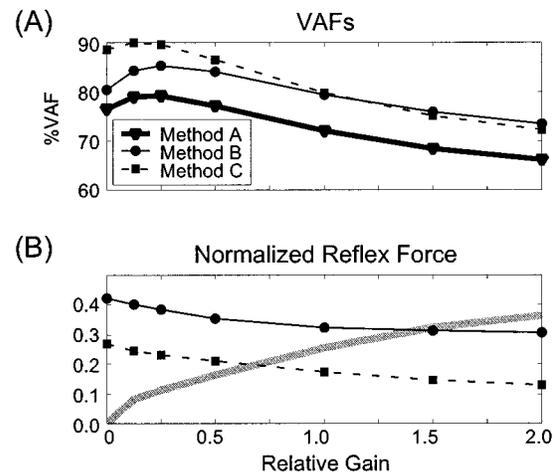


Fig. 5. Identification results for the cat soleus model. (A) The variance accounted for by each identification algorithm. (B) Standard deviation of the actual muscle force (thick gray line) for these simulations and that estimated by the two nonlinear algorithms. Reflexively generated muscle force is normalized with respect to the total muscle force.

reflex contributions for this particular system. The estimated stiffness parameter increased while the viscosity decreased with increasing reflex gain, leading to errors of 9% and 56%, respectively, at a normalized reflex gain of 1.0.

### C. Cat Soleus Model

Fig. 5 summarizes the ability of each identification algorithm to characterize the simulated cat soleus force data. Part (A) shows the VAF by each algorithm. All identification algorithms showed similar trends with respect to how accurately they described the simulated muscle force. VAF peaked for all methods at a relative reflex gain of approximately 0.2 and decreased by 10%–15% for further increases. For all gains, Methods B and C accounted for approximately 10% more of the simulated data variance than did Method A. Because the cat soleus model did not have explicit intrinsic stiffness and viscosity parameters to compare to the estimated values, the ability of Methods B and C to separate intrinsic and reflexively generated muscle forces was summarized differently for this set of simulations. Reflex contributions to net muscle force were estimated by subtracting the force response with no reflex feedback from those at all nonzero levels of reflex gain. This "reflexively" generated muscle force was then compared to the reflex force predicted by each of the identification algorithms. Fig. 5(B) compares the standard deviations of the estimated and simulated reflexively generated muscle forces, normalized by the standard deviation of the total muscle force. It is evident that neither Method B nor C successfully identified the reflex contribution to the total muscle response. Although the reflexes served to increase the force response to perturbations, both of these algorithms estimated a "reflexively" generated force contribution that decreased with increasing reflex gain.

### IV. DISCUSSION

In this study, we examined the use of system identification-based techniques for noninvasively characterizing the contribu-

tions of reflex properties to the stiffness of human joints. These techniques offer the promise of characterizing reflex properties during natural, functional conditions, thus avoiding physiological distortions due to methods that attempt to simply suppress reflex properties. The system identification-based techniques require assumptions regarding the structure of the reflex response, however, and several different assumptions have been made by different investigators. In this study, we used simulation methods to determine the impact of the structural assumptions made by two recently proposed system identification algorithms. Our results indicate that these methods perform extremely well if the structure of the reflex system is identical to that assumed by the system identification method. Not surprisingly, methods that make fewer assumptions regarding the structure of the system perform more accurately when used to characterize systems with different reflex structures. These results indicate that 1) system identification methods can indeed be used successfully to identify reflex properties during natural conditions and 2) either the structure of the reflex system must be known *a priori* or a general, flexible reflex structure must be assumed.

### A. Model Structure Assumptions

System identification algorithms based upon parameterized system models are very common in the field of control engineering and neuromuscular modeling [30], [36]–[39]. Often, the model structure can be concise because it is based on physiological understanding, and the model parameters have clear physical interpretations. Once a suitable model structure is chosen, identification of the model parameters can be very efficient, allowing for real-time identification. However, if the assumed model structure is not correct, the identified parameters will be computed to minimize output prediction error but will not be physiologically meaningful. For example, Method B provided incorrect intrinsic stiffness parameters for the ankle model, which had only a slightly different structure than assumed by the algorithm. These results illustrate that when model structure cannot be determined accurately or the "best" structure cannot be related to the underlying physiology, the utility of using a concise, physiology-based model is greatly diminished.

The other approach to separately identifying intrinsic and reflex properties described here is a block structured nonlinear nonparametric technique that makes fewer assumptions about system structure (Method C). The assumptions of this algorithm were that the intrinsic properties are linear, that the reflex delay is greater than the duration of the intrinsic dynamics, and that the reflex dynamics can be adequately characterized by a static nonlinearity followed by linear dynamics. No additional assumptions were made regarding the subsystems within this model. Rather, they were nonparametrically characterized using measurements of the system input and output. As would be expected, this identification routine worked well for the ankle simulations, which exactly matched the structure expected by the algorithm. In addition, it successfully separated the reflex and intrinsic contributions to the stretch response for the elbow model, which had a different reflex structure. This finding illustrates some generality associated with this approach. This gen-
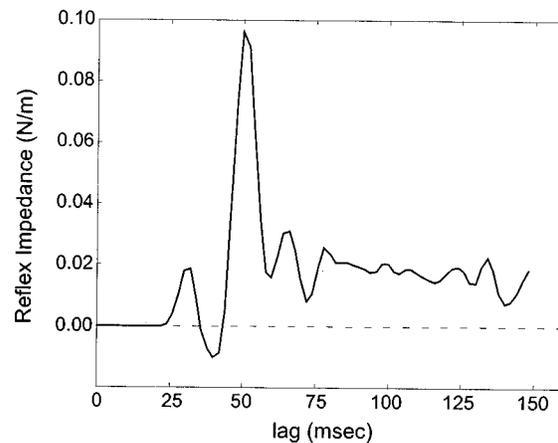


Fig. 6.   Nonparametrically estimated reflex IRF for the human elbow model. The reflex delay for this simulation was 50 msec. The input for this identification was joint velocity and the output was the residual joint torque not described by the estimated intrinsic muscle dynamics.

erality has other benefits, including the ability to provide information about incorrectly chosen structures. For example, Fig. 6, shows the reflex pathway IRF estimated by Method C using the simulated elbow model data. It describes the linear relationship between joint velocity and reflex torque, as shown in Fig. 1(C). This IRF returns to a nonzero steady-state, indicating that an integration operation is occurring. This behavior implies that the simulated elbow reflex [see Fig. 1(B)] has a position dependent component and that the assumption of only a velocity dependent pathway [Fig. 1(C)] is inappropriate for this particular system. In an experimental setting, the block structure of the nonparametric algorithm could be adapted to take this information into account. A careful analysis of the residuals can also be used to assess model validity in algorithms that incorporate either parametric or nonparametric subsystems, although these techniques will miss an incorrectly chosen structure that still adequately minimizes measurement output variance. Such situations can easily occur with over-parameterized systems or nonindependent signal pathways and can lead to erroneous physiological interpretations.

While Method C was able to characterize a more general class of systems than Method B, it was not able to accurately separate intrinsic and reflex contributions for the simulated cat soleus model. The primary assumption of Method C is that the intrinsic muscle dynamics decay before the onset of reflex activity. Fig. 7 shows the nonparametric step response for the intrinsic dynamics estimated from the simulated cat soleus data. It is evident that these dynamics do not decay before the onset of reflex activity, thereby violating the primary assumption of this algorithm. Again though, the incorporation of nonparametric subsystems provides insight to these performance limitations, which is not as readily accessible from the parametric approach.

### B. Practical Experimental Design

This work has significant implications for the successful design of experiments used to study reflex dynamics. Given the susceptibility of fully parametric algorithms to lead to erroneous physiological interpretations when the structure assumed
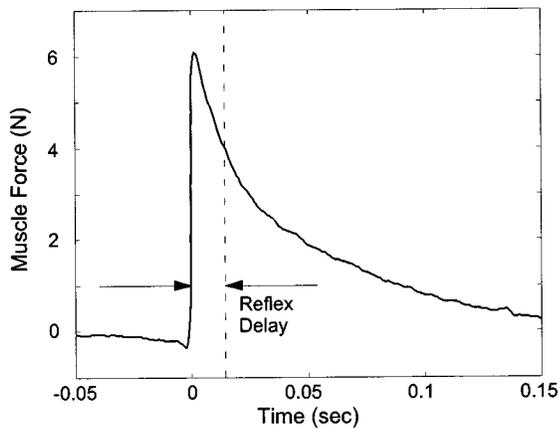
Fig. 7. Nonparametrically estimated step response for the cat soleus muscle. Response was estimated for a 1 mm step change in muscle length, while the gain of all reflex pathways was set to zero.

by the algorithm differs even slightly from the "true" system [e.g., Figs. 1(B) and (C)], the use of these techniques should be avoided unless the assumed structure is verified for *each* system to which it is applied. For a given task, reflex responses are likely to have significantly different properties at different joints (e.g., ankle and elbow) based upon the typical physiological role of the muscles crossing that joint and known differences in muscle spindle density. Even larger differences can be expected across species, where lower vertebrates are thought to rely more on reflex responses than higher vertebrates. In addition, reflex responses at a given joint are known to change with changes in task [40], [41], such as changes from an isometric to an isotonic state. Hence, the likelihood of successfully using a common reflex structure across different experimental preparations or even different paradigms in the same preparation is not certain. Instead, a new set of validation experiments needs to performed for each system studied.

## C. Reflex Simulation Models

Three models of the stretch reflex system were chosen for this simulation study. All were based on previously published experimental results, and all encapsulate at least some aspects of widely accepted properties of the stretch reflex response. The selection of models in this study invariably had a strong influence on the performance of the identification algorithms. Nevertheless, it does not influence the fundamental conclusions of this work. Based on the specific models chosen for simulation, Method B, which is fully parametric, appeared to be less robust than Method C, which incorporated nonparametric subsystems into its assumed structure. At least part of this result arises because the experimentally measured reflex response is much stronger at the human ankle than it is at the human elbow. This experimental result was also reflected in the chosen simulation models. For the joint perturbations used in this work, simulated reflexes at the elbow accounted for only 2.1% of the total joint torque variance, whereas those at the ankle accounted for 41% of the total torque. Therefore, even though the structure of the simulated elbow model was different than that presumed by Method C, the relatively small reflex contribution of this system

may have aided this algorithm in estimating constant intrinsic muscle parameters at all levels of simulated reflex gain. By contrast, the Method B had a more difficult task of identifying constant intrinsic dynamics for the simulated ankle model, which had a much stronger reflex contribution.

The absolute performance of these algorithms for the chosen simulation models is not of primary interest. Rather, the critical observation is that an incorrect choice of model structure can lead to incorrect physiological interpretations, independent of the identification strategy used. Hence, it is evident that successfully applying the tools of nonlinear system identification to the study of the stretch reflex response requires a careful assessment of the appropriate model structure. The primary advantage of the nonparametric algorithms is that they provide some indication about the validity of the chosen structure. This information is not directly available from the results of a parametric system identification process, although tools do exist for choosing and validating model structure [42], [43] and should be used to validate any structures, especially those based upon *a priori* information from different experimental preparations.

## REFERENCES

[1] E. Bizzi, P. Dev, P. Morasso, and A. Polit, "Effect of load disturbances during centrally initiated movements," *J. Neurophys.*, vol. 41, pp. 542–556, 1978.

[2] G. E. Loeb, "Hard lessons in motor control from the mammalian spinal cord," *Trends in Neuroscience*, vol. 10, pp. 108–113, 1987.

[3] P. B. C. Matthews, "The knee jerk: Still an enigma?," *Can. J. Physiol. Pharmacol.*, vol. 68, pp. 347–354, 1990.

[4] G. C. Agarwal and G. L. Gottlieb, "Effect of vibration on the ankle stretch reflex in man," *Electroenceph., Clin. Neurophysiol.*, vol. 49, pp. 81–92, 1980.

[5] J. H. J. Allum, K.-H. Mauritz, and H. Vogele, "The mechanical effectiveness of short latency reflexes in human triceps surae muscles revealed by ischaemia and vibration," *Exp. Brain Res.*, vol. 48, pp. 153–156, 1982.

[6] T. Sinkjaer and R. Hayashi, "Regulation of wrist stiffness by the stretch reflex," *J. Biomech.*, vol. 22, pp. 1133–1140, 1989.

[7] T. Sinkjaer, E. Toft, S. Andreassen, and B. C. Hornemann, "Muscle stiffness in human ankle dorsiflexors: Intrinsic and reflex components," *J. Neurophys.*, vol. 60, pp. 1110–1121, 1988.

[8] R. R. Carter, P. E. Crago, and M. W. Keith, "Stiffness regulation by reflex action in the normal human hand," *J. Neurophys.*, vol. 64, pp. 105–118, 1990.

[9] J. W. Aldridge and R. B. Stein, "Nonlinear properties of stretch reflex studied in the decerebrate cat," *J. Neurophys.*, vol. 47, pp. 179–192, 1982.

[10] M. D. Binder, C. J. Heckman, and R. K. Powers, "The Physiological Control of Motoneuron Activity," in *Handbook of Physiology. Exercise: Regulation and Integration of Multiple Systems*, L. B. Rowell and J. T. Shepard, Eds. New York: Oxford Univ. Press, 1996, pp. 1–53.

[11] R. K. Powers and M. D. Binder, "Summation of motor unit tensions in the tibialis posterior muscle of the cat under isometric and nonisometric conditions," *J. Neurophysiol.*, vol. 66, pp. 1838–1846, 1991.

[12] T. I. H. Brown, P. M. H. Rack, and H. F. Ross, "Forces generated at the thumb interphalangeal joint during imposed sinusoidal movement," *J. Physiol.*, vol. 332, pp. 69–85, 1982.

[13] D. J. Bennett, "Stretch reflex responses in the human elbow joint during a voluntary movement," *J. Physiol.*, vol. 474, pp. 339–351, 1994.

[14] R. Stein, I. W. Hunter, S. R. Lafontaine, and L. A. Jones, "Analysis of short-latency reflexes in human elbow flexor muscles," *J. Neurophys.*, vol. 73, pp. 1900–1911, 1995.

[15] R. B. Stein and R. E. Kearney, "Nonlinear behavior of muscle reflexes at the human ankle joint," *J. Neurophys.*, vol. 73, pp. 65–72, 1995.

[16] R. E. Kearney, R. B. Stein, and L. Parameswaran, "Identification of intrinsic and reflex contributions to human ankle stiffness dynamics," *IEEE Trans. Biomed. Eng.*, vol. 44, pp. 493–504, June 1997.

[17] L.-Q. Zhang and W. Z. Rymer, "Simultaneous and nonlinear identification of mechanical and reflex properties of human elbow joint muscles," *IEEE Trans. Biomed. Eng.*, vol. 44, pp. 1192–1209, Dec. 1997.

[18] E. J. Perreault, P. E. Crago, and R. F. Kirsch, "Simultaneous estimation of intrinsic and reflex contributions to muscle dynamics: A modeling study," *Proc. Int. Conf. IEEE/EMBS*, vol. 20, pp. 2346–2349, 1998.

[19] D. T. Westwick and R. E. Kearney, "Nonparametric identification of nonlinear biological systems, part I: Theory," *CRC Critical Reviews in Biomedical Engineering*, vol. 26, pp. 153–226, 1998.

[20] G. L. Gottlieb and G. C. Agarwal, "Dependence of human ankle compliance on joint angle," *J. Biomech.*, vol. 11, pp. 177–181, 1978.

[21] P. Weiss, R. E. Kearney, and I. W. Hunter, "Position dependence of ankle joint dynamics—II. Active dynamics," *J. Biomech.*, vol. 19, pp. 737–751, 1986.

[22] R. F. Kirsch, D. Boskov, and W. Z. Rymer, "Muscle stiffness during transient and continuous movements of cat muscle: Perturbation characteristics and physiological relevance," *IEEE Trans. Biomed. Eng.*, vol. 41, pp. 758–770, Aug. 1994.

[23] J. C. Houk, W. Z. Rymer, and P. E. Crago, "Dependence of dynamic response of spindle receptors on muscle length and velocity," *J. Neurophys.*, vol. 46, pp. 143–166, 1981.

[24] R. Poppele, "An analysis of muscle spindle behavior using randomly applied stretches," *Neuroscience*, vol. 6, pp. 1157–1165, 1981.

[25] Z. Hasan, "A model of spindle afferent response to muscle stretch," *J. Neurophys.*, vol. 49, pp. 989–1006, 1983.

[26] R. E. Kearney and I. W. Hunter, "System identification of human joint dynamics," *CRC Crit. Rev. Biomed. Eng.*, vol. 18, pp. 55–87, 1990.

[27] I. W. Hunter and M. J. Korenberg, "The identification of nonlinear biological systems: Wiener and Hammerstein cascade models," *Biol. Cybern.*, vol. 55, pp. 135–144, 1986.

[28] R. E. Kearney and I. W. Hunter, "Nonlinear identification of stretch reflex dynamics," *Ann. Biomed. Eng.*, vol. 16, pp. 79–94, 1988.

[29] G. C. Agarwal and G. L. Gottlieb, "Compliance of the human ankle joint," *J. Biomech. Eng.*, vol. 99, pp. 166–170, 1977.

[30] D. J. Bennett, J. M. Hollerbach, Y. Xu, and I. W. Hunter, "Time-varying stiffness of the human elbow joint during cyclic voluntary movement," *Exp. Brain Res.*, vol. 88, pp. 433–442, 1992.

[31] I. W. Hunter and R. E. Kearney, "Two-sided linear filter identification," *Med. Biol. Eng. Comput.*, vol. 21, pp. 203–209, 1983.

[32] C. C. Lin, "Neuromechanical interaction in the stretch reflex: A structural simulation model," in *Biomedical Engineering*. Cleveland, OH: Case Western Reserve Univ., 1997.

[33] T. R. Nichols and J. C. Houk, "Improvement in linearity and regulation of stiffness that results from actions of stretch reflex," *J. Neurophys.*, vol. 39, pp. 119–142, 1976.

[34] J. A. Hoffer and S. Andreassen, "Regulation of soleus muscle stiffness in premammillary cats: Intrinsic and reflex components," *J. Neurophys.*, vol. 45, pp. 267–285, 1981.

[35] A. Prochazka and P. St. J. Trend, "Instability in human forearm movements studied with feed-back-controlled muscle vibration," *J. Physiol.*, vol. 402, pp. 421–442, 1988.

[36] J. R. Dufresne, J. F. Soechting, and C. A. Terzuolo, "Reflex motor output to torque pulses in man: Identification of short- and long-latency loops with individual feedback parameters," *Neuroscience*, vol. 4, pp. 1493–1500, 1979.

[37] J. Winters and D. G. Kleweno, "Effect of initial upper-limb alignment on muscle contributions to isometric strength curves," *J. Biomech.*, vol. 26, pp. 143–153, 1993.

[38] R. Happee and F. C. T. Van Der Helm, "The control of shoulder muscles during goal directed movements, an inverse dynamic analysis," *J. Biomech.*, vol. 28, pp. 1179–1191, 1995.

[39] J. He, "Stretch reflex sensitivity: Effects of postural and muscle length changes," *IEEE Trans. Rehab. Eng.*, vol. 6, pp. 182–189, Feb. 1998.

[40] K. Akazawa, T. E. Milner, and R. B. Stein, "Modulation of reflex EMG and stiffness in response to stretch of human finger muscle," *J. Neurophys.*, vol. 49, pp. 16–27, 1983.

[41] C. Capaday and R. B. Stein, "Amplitude modulation of the soleus H-reflex in the human during walking and standing," *J. Neurosci.*, vol. 6, pp. 1308–1313, 1986.

[42] R. Haber and H. Unbehauen, "Structure identification of nonlinear dynamic systems—A survey of input/output approaches," *Automatica*, vol. 26, pp. 651–677, 1990.

[43] S. A. Billings and Q. M. Zhu, "Model validation tests for multivariable nonlinear models including neural networks," *International Journal of Control*, vol. 62, pp. 749–766, 1995.

**Eric J. Perreault** (S'97–M'00) received the B.Eng. and M.Eng. degrees in electrical engineering from McGill University, Montreal, Canada, in 1989 and 1992, respectively, and the Ph.D. in biomedical engineering from Case Western Reserve University, Cleveland, OH, in 2000.

From 1993 to 1995, he worked in industry as a Control Systems and Design Engineer. Currently, he is a Postdoctoral fellow in the Department of Physiology at Northwestern University Medical School, Chicago, IL. His research focuses on the neural control of movement, task-dependent strategies for neural control, muscle mechanics, and system identification of physiological systems.
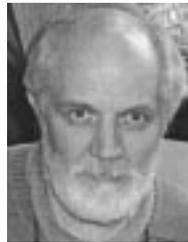
**Patrick E. Crago** (S'66–M'67) received the B.S. degree in electrical engineering from Carnegie-Mellon University, Pittsburgh, PA, in 1967, and the M.S. and Ph.D. degrees in biomedical engineering from Case Western Reserve University (CWRU), Cleveland, OH, in 1970 and 1973, respectively. He did post-doctoral studies in neuromuscular physiology in the Department of Physiology at Johns Hopkins University, Baltimore, MD.

He returned to CWRU as a Senior Research Associate in 1976, and joined the biomedical engineering faculty in 1982 as an Assistant Professor. He was promoted to Associate Professor and Professor in 1987 and 1992, respectively. He is currently the Allen H. and Constance T. Ford Professor of Biomedical Engineering, and chairman of the department. His research interests are in restoration of movement by functional neuromuscular stimulation and in normal and pathological movement control and regulation. Current research projects include biomechanical, neural and neuroprosthetic control of the wrist, forearm and elbow, and the clinical implementation and evaluation of neuroprostheses for hand grasp and proximal arm control. His research is funded by the National Institutes of Health and the Department of Veterans Affairs. His research laboratory is located in the Rehabilitation Engineering Center at MetroHealth Medical Center, which is part of the Cleveland FES Center.

Dr. Crago is a member of the IEEE Engineering in Medicine and Biology Society, the American Society for Biomechanics, the Society for Neuroscience, the American Association for the Advancement of Science, and the International FES Society.

**Robert F. Kirsch** (S'80–M'82) received the B.S. degree from the University of Cincinnati, Cincinnati, OH, in 1982 and the M.S. and Ph.D. degrees from Northwestern University, Evanston, IL, in 1986 and 1990, respectively.

He completed a post-doctoral fellowship at McGill University, Montreal, PQ, Canada, in 1993. He is currently an Assistant Professor in the Department of Biomedical Engineering at Case Western Reserve University and a Biomedical Engineer at the Cleveland VA Medical Center. His research focuses on the neural control of movement, restoring movement through the use of functional neuromuscular stimulation, and musculoskeletal modeling of the human body.